Carbohydrate Polymers 282 (2022) 119134

Contents lists available at ScienceDirect

Carbohydrate Polymers

journal homepage: www.elsevier.com/locate/carbpol

Antifibrotic effect of brown algae-derived fucoidans on osteoarthritic fibroblast-like synoviocytes

María Piñeiro-Ramil [a], Noelia Flórez-Fernández [b], Olalla Ramil-Gómez [c,d], María Dolores Torres [b], Herminia Dominguez [b], Francisco J. Blanco [e,f], Rosa Meijide-Faílde [a,g], Carlos Vaamonde-García [h,*]

[a] Universidade da Coruña, Tissue Engineering and Cellular Therapy Group, Instituto de Investigación Biomédica de A Coruña (INIBIC), Centro de Investigaciones Científicas Avanzadas (CICA), 15006 A Coruña, Spain
[b] CINBIO, Universidade de Vigo, Biomass and Sustainable Development Group (EQ2), Departament of Chemical Engineering, 32004 Ourense, Spain
[c] Aging and Inflammation Research Laboratory, Instituto de Investigaciones Biomédicas de A Coruña (INIBIC), 15006 A Coruña, Spain
[d] Universidade de Coruña, Endocrine, Nutritional and Metabolic Diseases Group, Departamento de Fisioterapia, Medicina y Ciencias Biomédicas, Facultad de Ciencias de la Salud, 15006 A Coruña, Spain
[e] Universidade da Coruña, Grupo de Investigacion en Reumatología y Salud, Centro de Investigaciones Científicas Avanzadas (CICA), Departamento de Fisioterapia, Medicina y Ciencias Biomédicas, Facultad de Fisioterapia, 15006 A Coruña, Spain
[f] Hospital Universitario A Coruña, Instituto de Investigación Biomédica de A Coruña (INIBIC), Grupo de Investigacion en Reumatología, 15006 A Coruña, Spain
[g] Universidade da Coruña, Departamento de Fisioterapia, Medicina y Ciencias Biomédicas, Facultad de Ciencias de la Salud, 15006 A Coruña, Spain
[h] Universidade da Coruña, Grupo de Investigacion en Reumatología y Salud, Centro de Investigaciones Científicas Avanzadas (CICA), Departamento de Biología, Facultad de Ciencias, 15071 A Coruña, Spain

ARTICLE INFO

Chemical compounds studied in this article:
PubChem CID: 74873 3-(Trimethylsilyl) propane-1-sulfonic acid
PubChem CID: 24602 Deuterium oxide
PubChem CID: 92023653 Fucoidan
PubChem CID: 56842206 Transforming growth factor beta
PubChem CID: 44259 Staurosporine
PubChem CID: 145068 Nitric oxide
PubChem CID: 104981 Propidium iodide
PubChem CID: 75783 Picrosirius red
PubChem CID: 4784 Phenylmethylsulfonyl fluoride

Keywords:
Fucoidan
Transforming growth factor beta
Fibrosis
Synovial fibroblasts
Apoptosis
Nitric oxide

ABSTRACT

Synovial fibrosis is a pathological process which contributes to joint pain and stiffness in several musculoskeletal disorders. Fucoidans, sulfated polysaccharides found in brown algae, have recently emerged as promising therapeutic agents. Despite the increasing amount of evidence suggesting the protective role of fucoidans in different experimental approaches of human fibrotic disorders, the effect of these sulfated polysaccharides on synovial fibrosis has not been investigated yet. By an *in vitro* experimental approach in fibroblast-like synoviocytes, we detected that fucoidans inhibit their differentiation into myofibroblasts with tumor cell-like characteristics and restore apoptosis. Composition and structure of fucoidan appear to be critical for the detected activity. Furthermore, protective effects of these sulfated polysaccharides are mediated by upregulation of nitric oxide production and modulation of TGF-β/smad pathway. Altogether, our results support the use of fucoidans as therapeutic compounds in the treatment of the fibrotic processes involved in rheumatic pathologies.

Abbreviations: OA, osteoarthritis; FLS, fibroblast-like synoviocytes; ECM, extracellular matrix; Col, collagen; α-sma, alpha-smooth muscle actin 2; TFG-β, transforming growth factor-beta 1; NO, nitric oxide; DMEM, Dulbecco's modified Eagle's medium; FBS, fetal bovine serum; FF, fucoidan from *Fucus vesiculosus*; FM, fucoidan from *Macrocystis pyrifera*; FU, fucoidan from *Undaria pinnatifida*; stau, staurosporine; HPSEC, high performance size exclusion chromatography; NMR, nuclear magnetic resonance; col1a1, Type I collagen; col3a1, Type III collagen III; fn1, fibronectin 1; plod2b, procollagen-lysine 2-oxoglutarate 5-dioxygenase 2b; gapdh, glyceraldehyde 3-phosphate dehydrogenase; BrdU, 5-bromo-2′-deoxyuridine; PI, propidium iodide; ELISA, enzyme-linked immunosorbent assay; SEM, standard error of the mean; EMT, epithelial-mesenchymal transition.

* Corresponding author at: Facultad de Ciencias, Campus de Zapateira, 15071 A Coruña, Spain.
E-mail addresses: maria.pramil@udc.es (M. Piñeiro-Ramil), noelia.florez@uvigo.es (N. Flórez-Fernández), olalla.ramil.gomez@sergas.es (O. Ramil-Gómez), matorres@uvigo.es (M.D. Torres), herminia@uvigo.es (H. Dominguez), f.blanco1@udc.es, fblagar@sergas.es (F.J. Blanco), rosa.meijide.failde@udc.es (R. Meijide-Faílde), carlos.vaamonde.garcia@udc.es (C. Vaamonde-García).

https://doi.org/10.1016/j.carbpol.2022.119134
Received 12 November 2021; Received in revised form 23 December 2021; Accepted 9 January 2022
Available online 12 January 2022

1. Introduction

Rheumatic diseases are a group of heterogeneous pathologies characterized by the presence of inflammation and destruction in articular tissues (Vaamonde-García & López-Armada, 2019). Among them, osteoarthritis (OA) is the most prevalent chronic joint disorder, and a major source of pain, disability, and socioeconomic costs worldwide. A common feature of OA and other rheumatic diseases, such as rheumatoid arthritis, is the occurrence of a phenotypic alteration in the synovium, characterized by hyperplasia, leukocyte infiltration, neoangiogenesis, and, finally, fibrosis (Ciregia et al., 2021). In the synovial tissue, the fibrotic reaction involves an excess of collagen deposition which contributes to joint stiffness and pain (Hill et al., 2007; L. Zhang et al., 2021). Besides, OA is a risk factor for developing a fibrotic joint disorder known as arthrofibrosis, which can also be associated with joint trauma or surgery (Bierke et al., 2021).

Although it is widely known that chronic inflammation and tissue injury commonly favor fibrosis development, the exact mechanisms favouring the onset of this pathological event in the joints are still elusive. In synovial tissue fibrosis, phenotypic changes in fibroblast-like synoviocytes (FLS) are driven by their differentiation into myofibroblasts, cells that produce and secrete excessive levels of extracellular matrix (ECM) components, especially type I and type III collagen and fibronectin (Kasperkovitz et al., 2005; Schuster, Rockel, Kapoor, & Hinz, 2021; Steenvoorden et al., 2006). The hallmarks of fibroblast-to-myofibroblast transition are the expression of alpha-smooth muscle actin 2 (α-sma) and increased proliferation, migration and invasion capacities (Schuster et al., 2021).

Transforming growth factor-β1 (TGF-β) is the primary factor that drives fibrosis (Meng, Nikolic-Paterson, & Lan, 2016). TGF-β signaling is very complex; it is commonly accepted that ALK5-Smad2/3 signaling is responsible of its profibrotic effects, whereas ALK1-Smad1/5/8 pathway is involved in its antifibrotic action (Vaamonde-Garcia et al., 2019; Walton, Johnson, & Harrison, 2017). Nevertheless, opposite roles of these smad-based signaling pathways have also been described (Frangogiannis, 2020; Muñoz-Félix, González-Núñez, & López-Novoa, 2013). Nonetheless, TGF-β is also involved in many pivotal cellular processes (Ciregia et al., 2021). In the joint, TGF-β is typically associated with cartilage anabolism/anti-catabolism and has been recently shown to be correlated with clinically meaningful response to OA treatment (Watt et al., 2020). Therefore, TGF-β cannot be considered as a therapeutic target against fibrosis (Ciregia et al., 2021).

The development of effective antifibrotic therapies continues to be a research priority, as knowledge in this field is still quite limited and continues to progress slowly (Henderson, Rieder, & Wynn, 2020). Antioxidant therapy has been proposed as a new strategy for the prevention and treatment of fibrotic diseases (Luangmonkong et al., 2018; Varone, Gibiino, Gasbarrini, & Richeldi, 2019), and dietary supplementation with antioxidant-enriched products has already shown beneficial effects in liver and cystic fibrosis (Bae, Park, & Lee, 2018; Sagel et al., 2018). In this context, fucoidans, which are natural sulfated polysaccharides found in different species of brown algae, have gained special attention for its antioxidant and antitumor properties (Zayed & Ulber, 2019). These natural biomolecules have also shown anti-inflammatory, antiobesity and other health-promoting biological activities (Pradhan et al., 2020), and are thus considered attractive therapeutic alternatives for the treatment of different diseases. Consequently, the interest for the use of fucoidans in the food and pharmaceutical industry is rising fast (Zayed & Ulber, 2019).

Different factors influence in the biological properties of the fucoidan, such as composition, structure, presence and position of sulfate groups, and molecular weight, among others (Ferreira, Passos, Madureira, Vilanova, & Coimbra, 2015; Zayed, El-Aasr, Ibrahim, & Ulber, 2020). In addition, geographical location, season of collection, and extraction technology used have direct impact on their composition and structure, and hence in their properties. In the pursuit of promising therapeutic applications, a number of current studies about fucoidans have employed polysaccharides from commercial origin, such as compounds derived from *Undaria pinnatifida* and *Fucus vesiculosus* (Bittkau et al., 2019; Li et al., 2016). Interestingly, these fucoidans have demonstrated to attenuate activation of pathological pathways commonly leading to fibrosis (L. Wang et al., 2019; Wu et al., 2020). For example, fucoidans from *Fucus vesiculosus* and from *Laminaria japonica* have been shown to inhibit proliferation of tumor and non-tumor cell lines and to decrease the expression of ECM-associated proteins (Bittkau et al., 2019; H. Y. Chen et al., 2018).

However, despite growing evidence suggesting the antifibrotic role of fucoidans in different experimental approaches of human diseases, the impact of these sulfated polysaccharides on profibrotic phenotypic changes in FLS, as well as their therapeutic potential for arthrofibrosis treatment, have yet to be investigated. For these reasons, we evaluated the antifibrotic effect of fucoidans derived from *Fucus vesiculosus, Macrocystis pyrifera* and *Undaria pinnatifida* on TGF-β-activated OA FLS. In addition, we investigated the underlying molecular mechanisms implicated in this antifibrotic effect.

2. Materials and methods

2.1. Reagents and treatments

Fucoidans from the seaweed *Fucus vesiculosus* L. (FF), *Macrocystis pyrifera* L. (FM), and *Undaria pinnatifida* (FU), as well as TGFβ, were purchased to Sigma-Aldrich (San Luis, MO, USA). Primary FLS cultures were treated with 5, 30 and 100 μg/mL FF, FM, and FU, based on previous research (Ryu & Chung, 2016; Vaamonde-García et al., 2021). FLS were treated with fucoidans and in the presence of 10 ng/mL TGF-β in order to induce a fibrotic response (Ciregia et al., 2021; Remst et al., 2013; Vaamonde-Garcia et al., 2019). Staurosporine (stau; 1 μM) was employed as positive control of apoptosis.

2.2. Characterization of fucoidans

^{1}H NMR spectra of FF, FU and FM were recorded at least in triplicate using a ARX400 spectrometer (Bruker, Massachusetts, USA). Measurements were conducted using deuterium oxide as solvent and 3-(trimethylsilyl)-1-propane sulfonic acid (Sigma-Aldrich, Misuri, USA) as an internal standard, working at 75 °C and 400 MHz. Samples were dissolved in D_2O at 10 mg/mL. Peaks were identified following the protocol detailed elsewhere (Rasin et al., 2021).

The molar mass distribution of the fucoidans above was evaluated by High-Performance Size Exclusion Chromatography (HPSEC) with an HPLC (Agilent 1260, Germany) using a SuperMultipore PW-H column (6 mm × 15 cm) with a guard column SuperMP (PW)-H (4.6 mm × 3.5 cm), both from TSKgel by Tosoh Corporation (Japan). The HPLC was equipped with a refractive index (RI) detector. The mobile phase was Milli-Q water at 0.4 mL/min, and the temperature of the column was 40 °C. The standard used was polyethylene oxide at 786 kDa from Tosoh Corporation (Japan).

2.3. Cell culture

Synovial tissue was obtained from 10 OA patients (5 females and 5 males) who underwent joint replacement surgery and gave informed consent. The donors' median age was 75.6 [86.1–65.1] years old. This study was reviewed and approved by the Local Ethics Committee. FLS were isolated as previously described (Vaamonde-Garcia et al., 2019) and cultured in Dulbecco's modified Eagle's medium (DMEM) (Cambrex Bio Science, Baltimore, MD, USA) containing 10% fetal bovine serum (FBS), 2 mM L-glutamine, 100 mg/mL streptomycin, and 100 U/mL penicillin (all from Lonza, Basel, Switzerland). FLS were subcultured with trypsin-EDTA (Lonza) and were used for the experiments between the third and eighth passages. For RNA isolation, protein extraction, and

Table I
Primer sequences used for real-time qPCR assays.

Gene	Forward (5′-3′)	Reverse (5′-3′)
Collagen I *(col1a1)*	ctggccccattggtaatgt	accagggaaaccagtagcac
Collagen III *(col3a1)*	ctggaccccagggtcttc	catctgatccagggtttcca
Fibronectin 1 *(fn1)*	ctggccgaaaatacattgtaaa	ccacagtcgggtcaggag
Procollagen-lysine 2-oxoglutarate 5-dioxygenase 2b *(plod2b)*	cctgatatggctctttgccga	gggggctgagcatttggaat
Glyceraldehyde-3-phosphate dehydrogenase *(gapdh)*	agccacatcgctcagacac	gcccaatacgaccaaatcc

invasion assays, cells were seeded on 12-well plates (BD Biosciences, San Jose, CA, USA); for wound and apoptosis assays, on 24-well plates (BD Biosciences); for proliferation studies as well as nitric oxide (NO) and collagen levels measurements, on 96-well plates (BD Biosciences); and for immunocytochemistry analysis, on 8-well chamber slides (BD Biosciences). Prior to stimulation, quiescence was induced by incubating FLS in DMEM with 0.5% FBS overnight.

2.4. RNA isolation, reverse transcription and qPCR

After 48 h of stimulation with fucoidans and TGF-β, total RNA from FLS was extracted and purified using TRIzol Reagent (Invitrogen, Paisley, UK), chloroform (Sigma-Aldrich) and isopropanol (Sigma-Aldrich). The NZY First-Strand cDNA Synthesis Kit (Nzytech, Lisboa, Portugal) was employed for the synthesis of cDNA. Reverse transcription of 500 ng of RNA from each sample was carried out in a 96-Well Thermal Cycler (Applied Biosystems, Thermo Fisher Scientific, Madrid, Spain). cDNA products were then amplified by PCR using the Fast SYBR™ Green master mix (Roche Diagnostics, Abingdon, UK). Quantitative real-time polymerase chain reaction (qPCR) experiments were run on a LightCycler 480 instrument (Roche Diagnostics), employing LightCycler 480 SYBR Green I Master (Roche Diagnostics) and the primers shown in Table I. After analyzing the data with the LC480 software, version 1.5 (Roche Diagnostics), relative gene expression was calculated with the $2^{-\Delta\Delta CT}$ method. Glyceraldehyde-3-phosphate dehydrogenase (*gapdh*) was employed as the reference gene for normalization. All primers were purchased from Invitrogen.

2.5. Protein extraction, SDS-PAGE and Western blot

After 1 h of stimulation with fucoidans and TGF-β, intracellular proteins from FLS were extracted employing Tris-HCl buffer pH 7.5 with protease inhibitor cocktail and phenylmethylsulfonyl fluoride (all from Sigma-Aldrich). SDS-PAGE was performed as previously described (Vaamonde-Garcia et al., 2019) for proteins separation. After being transferred to membranes, proteins were incubated overnight at 4 °C with the following rabbit anti-human antibodies: anti-p-Smad2 (S465/467)/anti-p-Smad3 (S423/S425), anti-p-Smad1/5 (S463/465) (1:1000), and anti-Glyceraldehyde 3-phosphate dehydrogenase (GAPDH; 1:2500) (all from Cell Signaling Technology, Leiden, Netherlands). Anti-rabbit secondary antibody (1:1000, Dako, Germany) and ECL chemiluminescent substrate (Millipore, USA) were used for detecting antigen-antibody binding. Protein bands were quantified by densitometry with the ImageQ image processing software (http://imagej.nih.gov/). The band intensities of the proteins of interest were normalized to GAPDH band intensity for the same sample.

2.6. Cell proliferation assay

FLS were treated with 5 and 30 μg/mL FF, FM, and FU, with and without TGF-β, in DMEM with 2% FBS for 48 h. The BrdU Cell Proliferation Assay Kit (Cell Signaling Technology) was employed to evaluate the incorporation of 5-bromo-2′-deoxyuridine (BrdU) and thus cell proliferation, according to the manufacturer's instructions.

2.7. Cell wound assay

FLS were stimulated with 30 μg/mL FF, FM, and FU, with and without TGF-β, in DMEM with 0.5% FBS. After 48 h, a linear wound was produced by scratching cell monolayers with a 200 μL pipette tip. Subsequently, wells were washed twice with saline buffer (Fresenius Kabi, Barcelona, Spain) to remove the detached cells. Cells were observed with a Nikon Eclipse TS100 inverted microscope (Nikon Instruments Europe B.V., Amsterdam, Netherlands) photographed with a coupled XM Full HD digital camera (Hangzhou Xiongmai Technologies (XM), Hangzhou, China) just after scratching (day 0) and 24 h later (day 1). The ImageJ software was employed to assess the level of wound healing, which was calculated as the percentage of wound closure after 24 h.

2.8. Cell invasion assay

FLS were stimulated with 30 μg/mL FF, FM, and FU, with and without TGF-β, in DMEM with 0.5% FBS. After 48 h, cells were harvested and seeded on cell culture inserts with a pore size of 8 μm (Sarstedt, Nümbrecht, Germanay) previously coated with Matrigel (Corning, New York, USA). Cells were suspended in DMEM with 0.5% FBS to be seeded on the inserts, which were placed on a 24-well plate containing DMEM with 10% FBS. After 24 h of incubation, inserts were stained with crystal violet (Merck, Madrid, Spain). Invasive cells were visualized with a Nikon Eclipse TS100 inverted microscope and photographed with a coupled XM Full HD digital camera. Cell invasion was assayed using the ImageJ software to quantify the amount of invasive colonies.

2.9. Immunocytochemistry

After stimulation of cells with fucoidans in the presence or absence of TGF-β for 48 h, FLS were fixed with acetone for 10 min at 4 °C. After three washes in PBS, cells were permeabilized and blocked for 30 min in PBS with 0.1% Tween 20 and 1% BSA. After blocking, 1-hour incubation with a mouse anti-human α-sma primary antibody (1:500; DAKO A/S, Glostrup, Denmark) was performed at room temperature. After additional washes with 0.1% Tween 20 in PBS, cells were incubated with a peroxidase-labeled goat anti-mouse/rabbit secondary antibody (DAKO A/S) for 30 min and then counterstained with hematoxylin (Merck). An Olympus BX61 microscope coupled to an Olympus DP70 digital camera (Olympus Biosystems) was used to examine and photograph the slides. The percentage of stained area among FLS was measured with the ImageJ software.

2.10. Intracellular collagen quantification

Picrosirius red (PSR) staining (Sigma-Aldrich) (Junquiera, Junqueira, & Brentani, 1979) was employed to visualize and measure intracellular collagen, as previously describe (Vaamonde-Garcia et al., 2019). Briefly, after 48-hour stimulation, FLS were fixed in methanol, washed with PBS, stained with 0.1% PSR staining solution and washed with 0.1% acetic acid. Then, intracellular PSR staining was solubilized with 0.1 M sodium hydroxide. A Nanoquant Infinite M200 spectrophotometer (Tecan, Männedorf, Switzerland) was employed to measure absorbance at 550 nm.

2.11. Human pro-collagen I α1/COLIA1 assay

Collagen I is synthetized as a pro-collagen molecule. For this reason, the levels of collagen I in culture supernatants from cultured FLS after 48-hour treatment with 5 and 30 μg/mL FF, FM, and FU, with and without TGF-β, were determined employing the DuoSet ELISA kit for human pro-Collagen I α1 (R&D system), following the instructions of the manufacturer. Data were expressed as released picograms per mL. The working range was between 31.2 and 2000 pg/mL.

Table II
Ratio of fucose: sulfate of the fucoidans studied from *Fucus vesiculosus*, *Macrocystis pyrifera* and Undaria pinnatifida.

Ratio	Fucoidans from		
	Fucus vesiculosus	*Undaria pinnatifida*	*Macrocystis pyrifera*
Fucose:sulfate	1.00:0.81[c]	1.00:1.42[a]	1.00:1.25[b]

Standard deviations were lower than 1%. Data with different letters were significantly different ($p > 0.05$).

2.12. NO production assay

The Griess reaction was used to determine the effects of fucoidans on NO production in FLS after 48-hour treatment with TGF-β alone or together with 30 μg/mL FF, FM or FU. Briefly, 50 μL of culture supernatant were collected and mixed with 50 μL of Griess reagent for nitrite measurementsm and sodium nitrite was used as standard. A Nanoquant Infinite M200 spectrophotometer was employed to measure absorbance at 570 nm.

2.13. Apoptosis assay

The Annexin V method was used for the detection and measurement of apoptosis. FLS were treated for 48 h with TGF-β alone or together with 30 μg/mL FF, FM or FU. Staurosporine was employed as positive control of apoptosis. After that time, apoptosis was monitored by Annexin V/Propidium iodide (PI) assay (Immunostep, Salamanca, Spain), following the manufacturer's instructions, employing a FACSCalibur flow cytometer (Becton Dickinson, Mountain View, CA, USA). Briefly, Annexin V labeled with FITC was identified by green fluorescence and used to quantify apoptotic cells. Simultaneous staining with non-vital dye PI (which shows red fluorescence) allows the discrimination of intact cells (Annexin V-FITC negative, PI negative), early apoptotic cells (Annexin V-FITC positive, PI negative), late apoptotic cells (Annexin V-FITC positive, PI positive), and necrotic cells (Annexin V-FITC negative, PI positive). Apoptosis was calculated as percentage of apoptotic cells (including both early and late apoptosis) for each condition.

2.14. Statistical analysis

All data in the graphs are reported as points representing one single experiment with FLS obtained from one single patient, with standard error of the mean (SEM) to represent error. Means of the variables tested from "n" independent experiments (n = number of patients) is also shown in graphs. All results were analyzed using GraphPad Prism 5 software (GraphPad Software, San Diego, CA). The nonparametric Wilcoxon-test was used to compare different treatments; differences were considered as statistically significant when $p < 0.05$.

3. Results and discussion

3.1. Fucoidans attenuate FLS proliferation and differentiation into myofibroblasts

In a previous study, we detected that fucoidans from *Fucus vesiculosus*, *Macrocystis pyrifera*, and *Undaria pinnatifida* had antioxidant and anti-inflammatory effect on chondrocytes, while little effect was observed on synoviocytes. While trying to elucidate the relation between the composition and the protective effects of fucoidans, we found that anti-oxidant actions and concentration of fucose/sulfate seem critically relevant for fucoidan activity (Vaamonde-García et al., 2021). In this study, to further investigate the role of chemical properties and molecular weight in the biological properties of the fucoidans, we firstly analyzed the ratio fucose:sulfate. As shown in Table II, FU ratio was higher than that of FF and FM, with FU showing the highest sulfate concentration, and FM showing the lowest one. ^{1}H NMR spectra of FF and FM exhibited α-anomeric protons (5–5.6 ppm), ring protons (3.4–4.4), *O*-acetyl groups (~2.2 ppm) and methyl protons (1–1.3 ppm), whereas *O*-acetyl groups were not identified for FU spectrum (Fig. 1A). The highest values for the signal at the high-field region, which are characteristic for α-L-fucopyranoside residues, were identified for FM, followed by FF and FU. Similar regions were reportedly found in ^{1}H NMR spectra of other fucoidans from different brown seaweeds (Monsur, Jaswir, Simsek, Amid, & Alam, 2017; Rasin et al., 2021). It should be noteworthy that all tested fucoidans presented a similar molar mass distribution with a molecular weight above of >786 kDa (Fig. 1B).

Since we previously failed to observe a patent anti-inflammatory effect of fucoidans on synoviocytes, in the present study we evaluated if these sulfated polysaccharides were acting on fibrosis rather than inflammation. In order to explore this possibility, we established an *in vitro* model of profibrotic activation of FLS by stimulation with TGF-β (Ciregia et al., 2021; Vaamonde-Garcia et al., 2019). As shown in Fig. 2, TGF-β elicited a phenotypic change in FLS, promoting cell proliferation and inducing the expression of a classic myofibroblast marker, the

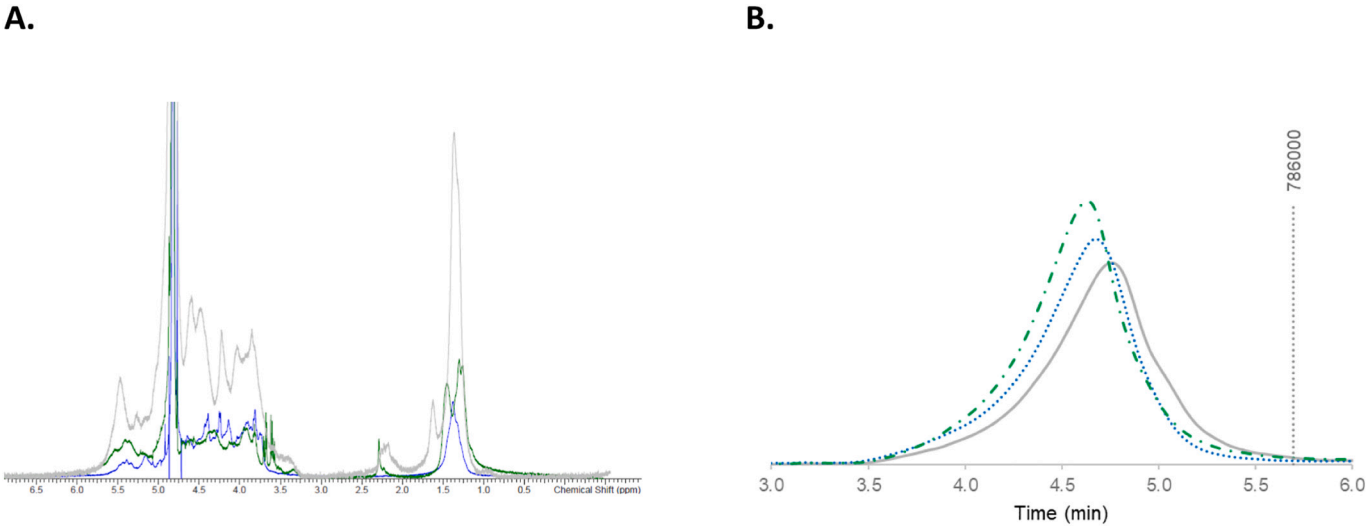

Fig. 1. Profiles of (**A**) ^{1}H NMR and (**B**) HPSEC of the fucoidans from *Fucus vesiculosus* (FF), *Undaria pinnatifida* (FU), and *Macrocystis pyrifera* (FM). Vertical dashed line indicates the weight of the pattern in dalton (Da). Symbols: FF (green line), FM (grey line) and FU (blue line). (For interpretation of the references to colour in this figure legend, the reader is referred to the web version of this article.)

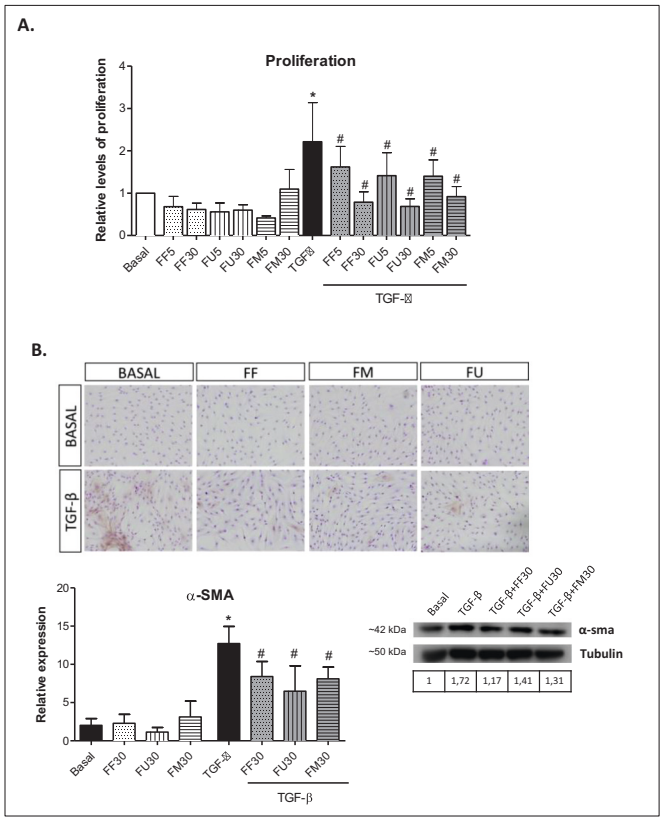

Fig. 2. Effect of fucoidans on FLS proliferation and differentiation into myofibroblast. FLS were incubated for 24 h with 5 or 30 μg/mL FF, FM, and FU, with or without TFG-β. Then, (**A**) cell proliferation was determined by BrdU assay ($n = 5$). (**B**) Alpha-smooth muscle actin 2 (α-sma) protein expression was assayed by immunohistochemistry and confirmed by western blot. Upper panel, representative images of cells stimulated as indicated and stained with α-sma. Left-lower panel, quantitative analysis of α-sma staining ($n = 3$). Original magnification: 100×. Right-lower panel, representative image of protein levels of α-sma analyzed by western blot and quantification shown on the bottom. Graphs represent means ± SEM. *, statistically different *vs.* basal condition ($p < 0.05$); #, statistically different *vs.* stimulated with TFG-β alone ($p < 0.05$); FLS, fibroblast-like synoviocytes; FF, fucoidan from *Fucus vesiculosus*; FM, fucoidan from *Macrocystis pyrifera*; FU, fucoidan from *Undaria pinnatifida*; TFG-β, transforming growth factor-beta 1.

protein α-sma. Interestingly, fucoidans reduced the proliferation induced by TGF-β in a dose-dependent manner (Fig. 2A). Likewise, the expression of α-sma was attenuated in those cells co-treated with fucoidans (Fig. 2B). Accordingly, previous studies showed that fucoidans reversed TGF-β-induced differentiation of fibroblasts into myofibroblasts, diminishing the expression of α-sma and reducing cell proliferation (H. Y. Chen et al., 2018; Y. Zhang, Du, Yu, & Zhu, 2020; Y. Zhang et al., 2018).

3.2. Fucoidans diminish the synthesis and release of ECM proteins induced by TFG-β

One of the events that characterize fibrosis is the accumulation of ECM proteins, mainly collagen, in the synovial tissue (Frangogiannis, 2020; Henderson et al., 2020). Likewise, α-sma-positive FLS are the main responsible for the production and secretion of ECM proteins, including fibrillar collagen (Frangogiannis, 2020; Henderson et al., 2020; Schuster et al., 2021). As expected, TGF-β-activated FLS showed increased expression of collagen I, collagen III, fibronectin, and procollagen-lysine, also known as 2-oxoglutarate 5-dioxygenase 2b (Plod2b) (Fig. 3). Plod2b is a gene involved in enzymatic increment of hydroxylated lysine residues within the telopeptides, contributing to increase pyridinoline cross-links in collagen deposits (Yamauchi & Sricholpech, 2012). This change in cross-linking is related to irreversible accumulation of collagen in fibrotic tissues (van der Slot et al., 2003). Likewise, previous studies indicated that upregulated expression of plod2b, and subsequent increase in pyridinoline cross-links, is the cause of the persistent fibrosis both in synoviocytes stimulated with TGF-β *in vitro* and in *in vivo* models of experimental OA (Remst et al., 2013; Remst, Blaney Davidson, & van der Kraan, 2015).

In our study, co-incubation of FLS with fucoidans reduced the gene expression of collagen I and III and fibronectin, the highest dose being generally more effective (Fig. 3A-C). Accordingly, treatment with similar concentrations of fucoidans reduced the expression of collagen I and α-sma in a model of radiation-induced fibrosis in fibroblasts, where modest inhibition of fibronectin expression was also detected (Wu, Chen, Tsai, Hsu, & Hwang, 2020). Moreover, different studies reported that fucoidans downregulate α-sma, col1a1, fibronectin and vimentin protein levels in TGFβ-induced cells (H. Y. Chen et al., 2018; J. Chen et al., 2015). However, in our study, these sulfated polysaccharides failed to modulate the expression of plod2b (Fig. 3D).

These results were confirmed at the protein level by intracellular collagen staining and measurement of type I collagen released to cell supernatant (Fig. 4). FLS co-treated with TGF-β and either FF or FM showed a reduction of intracellular collagen levels, which are raised by TGF-β, as indicated by PSR staining (Fig. 4A). Besides, the amount of type I pro-collagen in the culture media was significantly increased in those FLS stimulated with TGF-β, but co-incubation with FF, FU and FM strongly diminished its release (Fig. 4B). Accordingly, oligo-fucoidan treatment significantly reduced collagen accumulation in a model of renal tubulointerstitial fibrosis in mice (C. H. Chen et al., 2017). Interestingly, fucoidan produced by *Laminaria japonica*, which presents a percentage of fucose and sulfate similar to those of FF, FU and FM, but a lower molecular weight, attenuated interstitial and perivascular fibrosis, reducing collagen content and expression of ECM components in an animal model of diabetic cardiopathy (Yu et al., 2014). Taken together, these findings suggest that fucoidans' chemical composition plays a pivotal role in their antifibrotic effects.

3.3. Fucoidans attenuate TFG-β-elicited cell migration and invasion

Following TGF-β-induced activation, FLS acquire tumor cell-like characteristics such as impaired apoptosis, unlimited proliferation, and migration and invasion abilities. Regarding the latter processes, FLS can directly migrate and invade into the articular tissues surrounded by the synovium, so that a progressive degradation of articular cartilage and bone take place, exacerbating joint damage (Shu, Shi, Nie, & Guan, 2015; Yan et al., 2016). As shown in Fig. 5, TFG-β promoted FLS migration and invasion. Treatment with FF, FU or FM attenuated, although not significantly, the migration capacity of TFG-β-activated FLS, being FM the fucoidan which showed the clearest effect (Fig. 5A). All three fucoidans also diminished cell invasion induced by TFG-β, and again significant differences were found between FLS treated with FM and those treated with TGF-β alone (Fig. 5B). Similarly, a previous study using FLS derived from rheumatoid arthritis patients showed that fucoidans reduced invasiveness of IL-1β-treated cells (Shu et al., 2015). In a similar way, fucoidan from *Fucus vesiculosus* inhibited cell migration and invasion activity from human lung cancer cells *in vitro* (Lee, Kim, & Kim, 2012).

3.4. Fucoidans induce apoptosis and stimulate NO production

Evasion or impairment of apoptosis activation favors persistent fibroblasts differentiation into cells with a profibrotic phenotype, thus preventing fibrosis resolution (Hinz & Lagares, 2020). Interestingly, when apoptosis was evaluated in our *in vitro* model of synovial fibrosis, we observed that TFG-β downregulated cell apoptosis (Fig. 6A). Co-

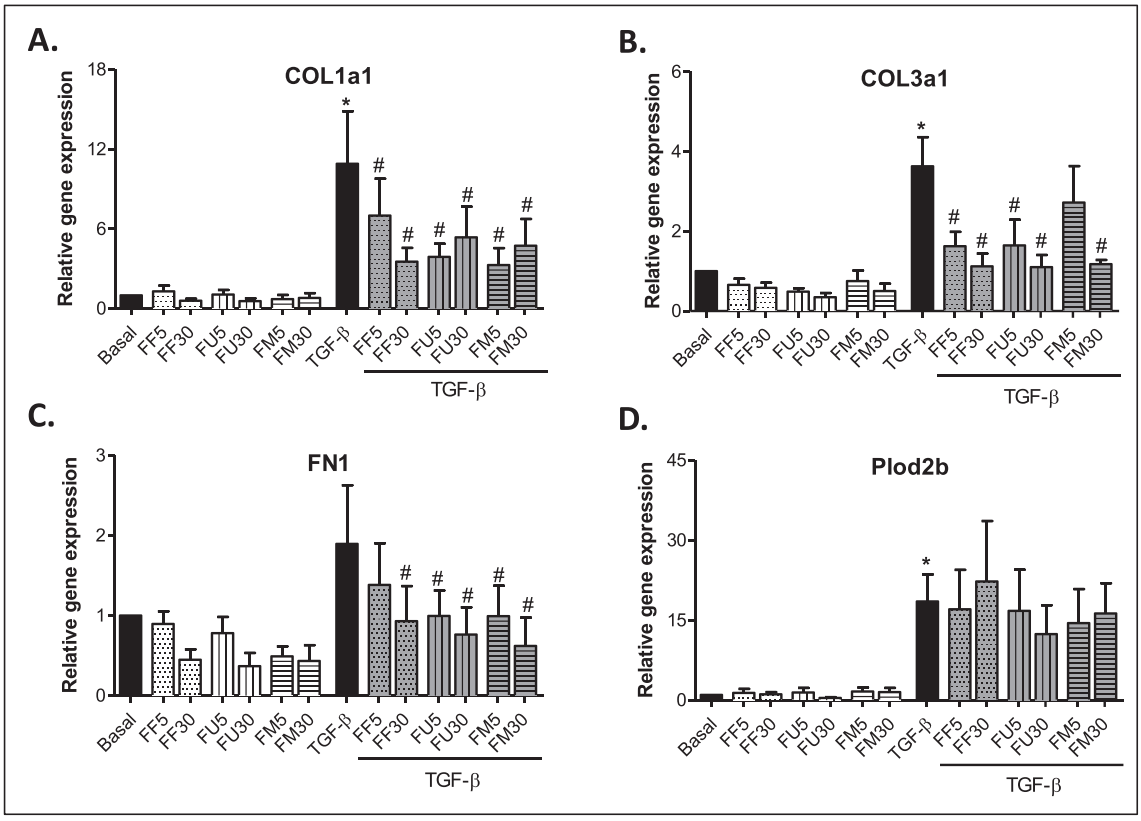

Fig. 3. Effect of fucoidans on gene expression of extracellular matrix proteins induced by TFG-β. FLS were stimulated for 48 h with FF, FM or FU, with or without TGF-β. Then, gene expression of collagen I (*col1a1*), collagen III (*col3a1*), fibronectin 1 (*fn1*), and procollagen-lysine 2-oxoglutarate 5-dioxygenase 2b (*plod2b*) was analyzed by RT-qPCR. Reference gene glyceraldehyde-3-phosphate dehydrogenase (*gapdh*) was used for normalizing gene expression ($n = 5$). Graphs represent means ± SEM. *, statistically different *vs.* basal condition ($p < 0.05$); #, statistically different *vs.* stimulated with TFG-β alone ($p < 0.05$); FLS, fibroblast-like synoviocytes; FF, fucoidan from *Fucus vesiculosus*; FM, fucoidan from *Macrocystis pyrifera*; FU, fucoidan from *Undaria pinnatifida*; TFG-β, transforming growth factor-beta 1.

incubation of FLS with FF, FU and FM attenuated this effect and allowed the recovering of basal levels of apoptosis, whose values were far lower from those obtained with positive control staurosporine. In a similar way, fucoidans have been described to induce apoptosis in different types of cancer cells (Lin et al., 2020). For instance, fucoidans from *Fucus vesiculosus* induce apoptosis and inhibit epithelial-mesenchymal transition (EMT) in breast cancer cells (He et al., 2019). Besides, in a previous study, Shu et al. (2015) observed that fucoidans activate apoptosis in rheumatoid arthritis FLS stimulated with IL-1β, thus exerting anti-survival activities on pathological synoviocytes (Shu et al., 2015).

Evidence indicates that the pro-apoptotic effects of these sulfated polysaccharides could be mediated by NO release (Jin, Song, Kim, Park, & Kwak, 2010; Takeda et al., 2012). Since it is known that NO induces apoptosis in OA synoviocytes (Borderie et al., 1999), we evaluated if FF, FU and FM could activate the production of NO in our model. As shown in Fig. 6B, the treatment with all three fucoidans reversed the inhibition of NO release induced by TFG-β. These findings suggest that the induction of NO production by fucoidans could participate in their pro-apoptotic effects and therefore in the amelioration of fibrosis. Likewise, Li et al. (2016) observed that fucoidans protect against liver fibrosis through inhibition of autophagy (Li et al., 2016), a physiological process in which damaged or unnecessary organelles are destroyed, and which is now considered a target for the prevention of synovial fibrosis (Maglaviceanu, Wu, & Kapoor, 2021). Since it is widely recognized that there is a crosstalk between apoptosis and autophagy (Fairlie, Tran, & Lee, 2020), the role of autophagy in the antifibrotic effect of fucoidans should not be discarded and future investigation are warranted.

3.5. Fucoidans modulate TFG-β-induced smad signaling

Smad signaling plays a central role in downstream pathways involved in TGF-β-induced activation of fibrosis (Hu et al., 2018). Two receptors are involved in these intracellular pathways: ALK5, which mediates phosphorylation of Smad2/3; and ALK1, which mediates phosphorylation of Smad1/5/8. In this study, we analyzed the levels of pSmad2/3 and pSmad1/5 as a measure of the activation of these pathways. As expected, TFG-β-stimulated cells showed phosphorylation of smad 2/3 and smad 1/5 (Fig. 7). Interestingly, all three fucoidans modulated these TFG-β signaling pathways in a different way. Fucoidan from *Fucus vesiculosus* significantly reduced pSmad 2/3 levels, whereas FM and FU failed to exert a consistent inhibitory effect (Fig. 7A-B). Conversely, phosphorylation of smad 1/5 was only significantly upregulated by fucoidan from *Macrocystis pyrifera* (Fig. 7A-C).

In a previous study, a fucoidan with a similar fucose:sulfate ratio (29% fucose: 30% sulfate) ameliorated fibrosis both *in vivo* and *in vitro*, at least partially through inhibiting smad3 phosphorylation and TGF-β signaling (J. Chen et al., 2015). Similarly, fucoidan from *Fucus vesiculosus* has been shown to suppress the upregulation of phosphorylated Smad2/3 induced by TGF-β, protecting retinal epithelial cells and hepatic stellate cells against EMT (Y. Zhang et al., 2018) in an *in vivo* model of liver fibrosis (Li et al., 2016). Additionally, beneficial effects of fucoidans have been also associated to upregulation of pSmad 1/5 levels and smad1-dependent smad 7 expression (Chale-Dzul, Pérez-Cabeza de Vaca, Quintal-Novelo, Olivera-Castillo, & Moo-Puc, 2020; Kim, Kang, Park, & Lee, 2015). Nonetheless, fucoidan from seaweed *Nemacystus decipiens* disrupts angiogenesis by blocking pSmad 1/5/8 signaling (W. Wang et al., 2016). Therefore, future studies will be needed in order to elucidate the precise role of smads in the protective effects of fucoidans.

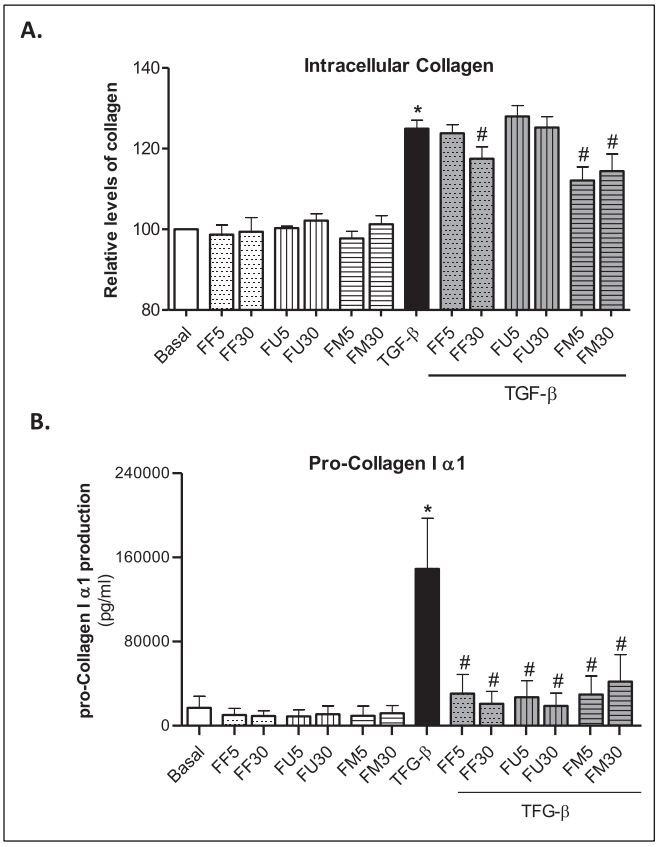

Fig. 4. Fucoidan modulation of protein collagen expression induced by TFG-β in FLS. FLS were stimulated for 48 h with FF, FM or FU, with or without TGF-β. Then, (**A**) levels of total intracellular collagens were analyzed by picrosirius red (PSR) stanning ($n = 5$). (**B**) Pro-collagen I α1 released in the culture supernatant was quantified by ELISA (n = 5). Graphs represent means ± SEM. *, statistically different *vs.* basal condition ($p < 0.05$); #, statistically different *vs.* stimulated with TFG-β alone ($p < 0.05$); FLS, fibroblast-like synoviocytes; FF, fucoidan from *Fucus vesiculosus*; FM, fucoidan from *Macrocystis pyrifera*; FU, fucoidan from *Undaria pinnatifida*; TFG-β, transforming growth factor-beta 1. (For interpretation of the references to colour in this figure legend, the reader is referred to the web version of this article.)

Taken together, these results suggest that these sulfated polysaccharides exert their antifibrotic actions in different ways, at least in terms of modulation of TFG-β/Smad signaling. Distinct chemical composition and structure among fucoidans could explain this phenomenon and thereby their different capacities to attenuate fibrosis-related processes such as cell invasion and ECM overproduction.

3. Conclusions and future perspectives

Collectively, our results indicate the antifibrotic effect of fucoidans on activated synoviocytes. This effect is mediated by the inhibition of fibroblast-to-myofibroblast transition, which leads to the upregulation of ECM production and the acquisition of tumor cell-like characteristics such as unlimited proliferation, migration and invasion abilities, and impaired apoptosis. Regarding the latest, fucoidans induce NO production and release, which is likely to activate the programmed cell death of pathological fibroblasts, thereby attenuating synovial fibrosis. Furthermore, the protective action of these sulfated polysaccharides is differently mediated by the modulation of TGF-β1/Smad pathways.

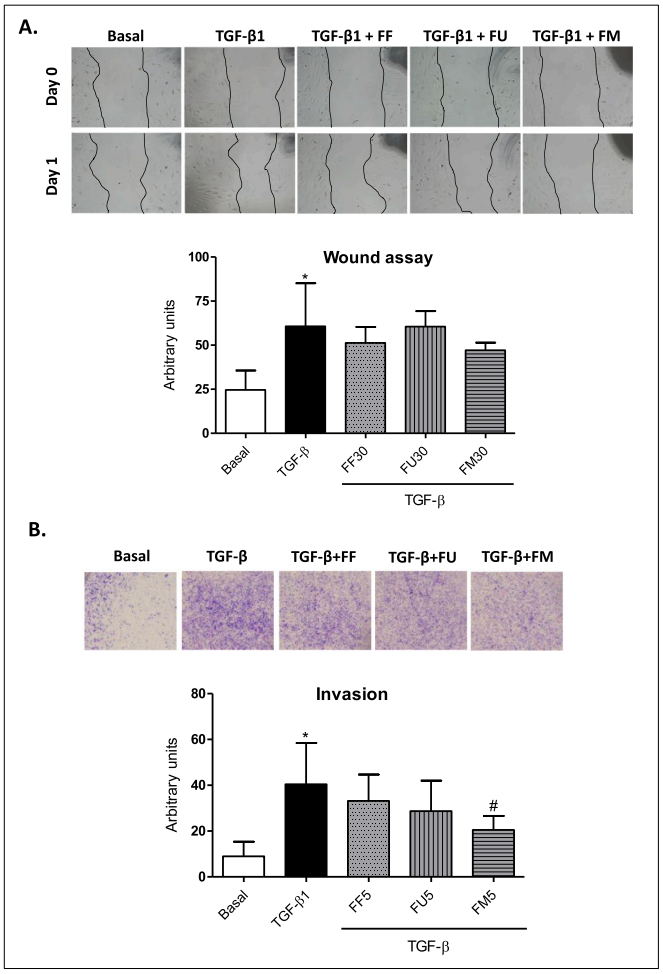

Fig. 5. Effect of fucoidans on cell migration and invasion in TFG-β-activated FLS. FLS were stimulated for 48 h with FF, FM or FU, with or without TGF-β. Then, (**A**) wound healing assays were performed. Upper panel, representative images showing cell monolayers just after wounding (day 0) and 24 h later (day 1). Original magnification: 40×. Lower panel, quantitative analysis of wound closure. Complete wound closure = 100% ($n = 5$). (**B**) Invasion assays were performed. Upper panel, representative images of crystal violet-stained invasive FLS after different treatments. Original magnification: 6.7×. Lower panel, quantitative analysis of crystal violet staining after invasion assay ($n = 4$). Graphs represent means ± SEM. *, statistically different *vs.* basal condition ($p < 0.05$); #, statistically different *vs.* stimulated with TFG-β alone ($p < 0.05$); FLS, fibroblast-like synoviocytes; FF, fucoidan from *Fucus vesiculosus*; FM, fucoidan from *Macrocystis pyrifera*; FU, fucoidan from *Undaria pinnatifida*; TFG-β, transforming growth factor-beta 1. (For interpretation of the references to colour in this figure legend, the reader is referred to the web version of this article.)

Overall, these findings along with those from our previous work (Vaamonde-García et al., 2021) and from other authors support the use of these marine polysaccharides as therapeutic agents in the treatment of rheumatic pathologies. Additionally, the findings here presented encourage the development of further studies targeting the composition and structure of fucoidans, as well as their relation with their biological properties. Hereby, clinical trials should also be developed in the pursuit of therapeutic applications of fucoidans which have already shown promising effects in *in vitro* approaches.

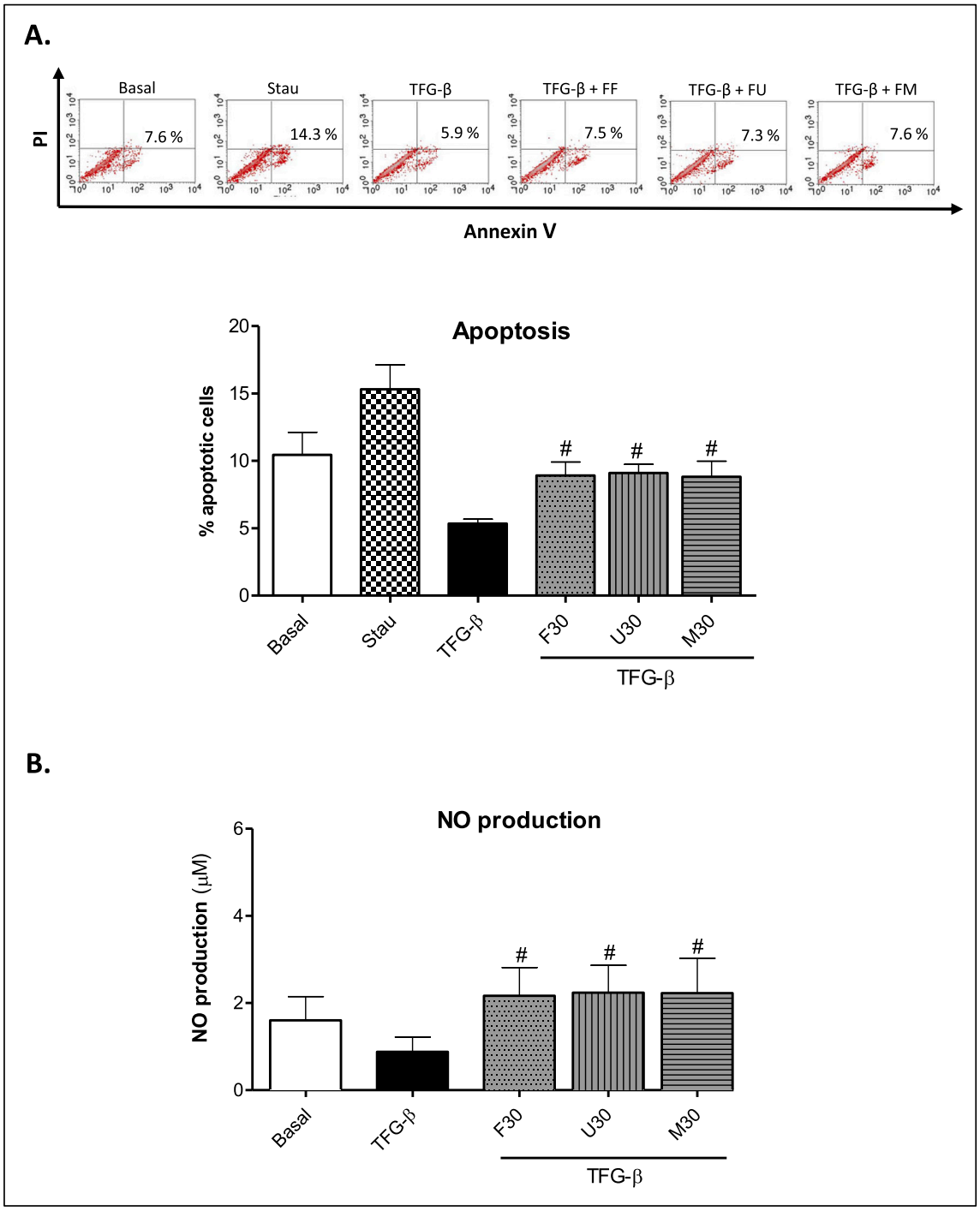

Fig. 6. Fucoidan recovery of apoptosis and NO production in TFG-β-activated FLS. FLS were stimulated for 48 h with TGF-β alone or together with FF, FM or FU. Staurosporine was employed as positive control. Then, (**A**) apoptosis was evaluated by flow cytometry. Upper panel, representative histograms from one experiment showing distribution of cell population and percentage of apoptotic cells (Annexin V and FITC positive). Lower panel, quantitative analysis of percentage of cells under apoptosis per condition ($n = 4$). (**B**) NO production was evaluated by Griess reaction (n = 4). Graphs represent means ± SEM. #, statistically different *vs.* stimulated with TFG-β alone ($p < 0.05$); FLS, fibroblast-like synoviocytes; FF, fucoidan from *Fucus vesiculosus*; FM, fucoidan from *Macrocystis pyrifera*; FU, fucoidan from *Undaria pinnatifida*; TFG-β, transforming growth factor-beta 1; Stau, staurosporine.

CRediT authorship contribution statement

María Piñeiro-Ramil: Formal analysis and Investigation, Writing – review & editing. **Noelia Flórez-Fernández:** Formal analysis and Investigation, Writing – review & editing. **Olalla Ramil-Gómez:** Formal analysis and Investigation, Writing– review & editing. **María Dolores Torres:** Formal analysis and Investigation, Writing– review & editing. **Francisco J Blanco:** Writing – review & editing. **Herminia Domínguez:** Writing – review & editing. **Rosa Meijide-Faílde:** Writing – review & editing. **Carlos Vaamonde-García**: Conceptualization, Formal analysis and Investigation, Supervision, Writing – review & editing.

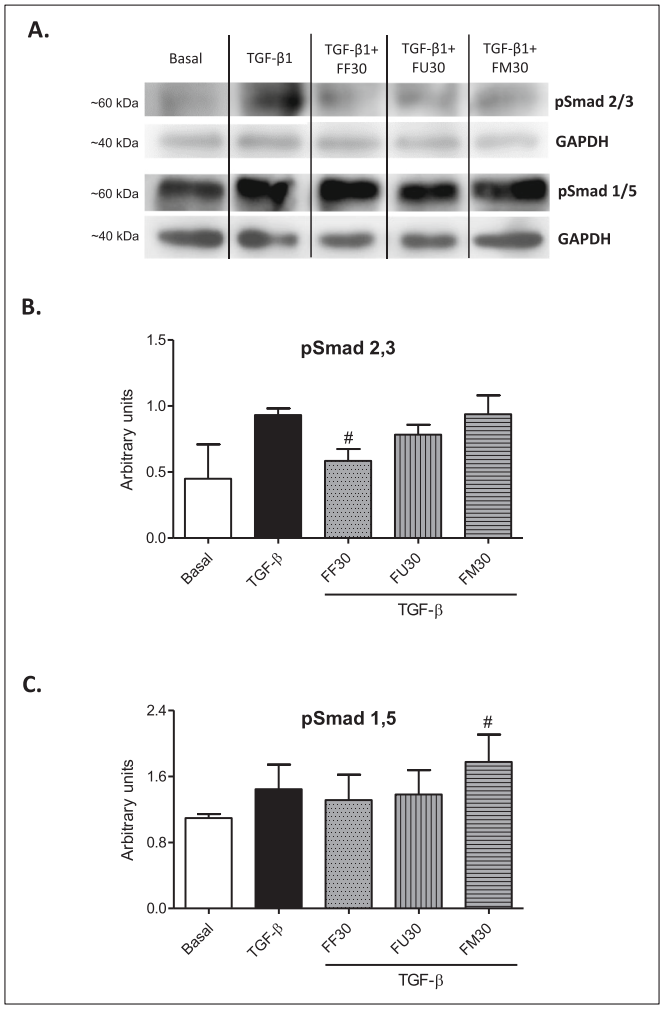

Fig. 7. Effect of fucoidans on phosphorylated levels of Smad 2/3 and Smad 1/5 in TFG-β-activated FLS. Cells were stimulated for 1 h with or without TGF-β alone or together with FF, FM or FU. (**A**) Representative images of western blot analysis from one experiment showing expression of pSmad 2/3, pSmad 1/5, and GAPDH. (**B**) Quantitative analysis of pSmad 2,3 levels ($n = 3$). (**C**) Quantitative analysis of pSmad 1,5 levels (n = 3). Graphs represent means ± SEM. #, statistically different *vs.* stimulated with TFG-β alone ($p < 0.05$); FLS, fibroblast-like synoviocytes; FF, fucoidan from *Fucus vesiculosus*; FM, fucoidan from *Macrocystis pyrifera*; FU, fucoidan from *Undaria pinnatifida*; TFG-β, transforming growth factor-beta 1.

Declaration of competing interest

The authors declare that they have no known competing financial interests or personal relationships that could have appeared to influence the work reported in this paper.

Acknowledgements

We are would like to thank the donors, medical staff and colleagues from CHUAC for providing the clinical samples. We are also grateful for the support and assistance from the laboratory CICA-INIBIC laboratory staff. Graphical abstract was created using images from SMART Servier Medical Art (smart.servier.com).

Funding sources

Financial support from the Xunta de Galicia and the European Union (European Regional Development Fund - ERDF) is gratefully acknowledged (Grupos con Potencial de Crecemento 2020, grant number ED431B 2020/55; Centro Singular de Investigación de Galicia 2019–2022, grant number ED431G2019/06; Rede Galega de Terapia Celular 2016, grant number R2016/036). N.F.-F. thanks Xunta de Galicia for her postdoctoral contract [grant number ED481B 2018/071]. M.D.T. thanks Ministry of Economy and Competitiveness of Spain for her postdoctoral grant [grant number RYC2018-024454-I]. C.V.-G. thanks Xunta de Galicia for his postdoctoral contract [grant number ED481D 2017/023]. Authors also thank Universidade da Coruña/CISUG for funding open access charge.

References

Bae, M., Park, Y. K., & Lee, J. Y. (2018). Food components with antifibrotic activity and implications in prevention of liver disease. *The Journal of Nutritional Biochemistry, 55*, 1–11.

Bierke, S., Abdelativ, Y., Hees, T., Karpinksi, K., Häner, M., Park, H., & Petersen, W. (2021). Risk of arthrofibrosis in anatomical anterior cruciate ligament reconstruction: The role of timing and meniscus suture. *Archives of Orthopaedic and Trauma Surgery, 141*(5), 743–750.

Bittkau, K. S., Dörschmann, P., Blümel, M., Tasdemir, D., Roider, J., Klettner, A., & Alban, S. (2019). Comparison of the effects of fucoidans on the cell viability of tumor and non-tumor cell lines. *Marine Drugs, 17*(8).

Borderie, D., Hilliquin, P., Hernvann, A., Lemarechal, H., Menkes, C. J., & Ekindjian, O. G. (1999). Apoptosis induced by nitric oxide is associated with nuclear p53 protein expression in cultured osteoarthritic synoviocytes. *Osteoarthritis and Cartilage, 7*(2), 203–213.

Chale-Dzul, J., Pérez-Cabeza de Vaca, R., Quintal-Novelo, C., Olivera-Castillo, L., & Moo-Puc, R. (2020). Hepatoprotective effect of a fucoidan extract from Sargassum fluitans borgesen against CCl. *International Journal of Biological Macromolecules, 145*, 500–509.

Chen, C. H., Sue, Y. M., Cheng, C. Y., Chen, Y. C., Liu, C. T., Hsu, Y. H., … Chen, T. H. (2017). Oligo-fucoidan prevents renal tubulointerstitial fibrosis by inhibiting the CD44 signal pathway. *Scientific Reports, 7*, 40183.

Chen, H. Y., Huang, T. C., Lin, L. C., Shieh, T. M., Wu, C. H., Wang, K. L., … Hsia, S. M. (2018). Fucoidan inhibits the proliferation of leiomyoma cells and decreases extracellular matrix-associated protein expression. *Cellular Physiology and Biochemistry, 49*(5), 1970–1986.

Chen, J., Cui, W., Zhang, Q., Jia, Y., Sun, Y., Weng, L., … Yang, B. (2015). Low molecular weight fucoidan ameliorates diabetic nephropathy via inhibiting epithelial-mesenchymal transition and fibrotic processes. *American Journal of Translational Research, 7*(9), 1553–1563.

Ciregia, F., Deroyer, C., Cobraiville, G., Plener, Z., Malaise, O., Gillet, P., … de Seny, D. (2021). Modulation of α. *Experimental & Molecular Medicine, 53*(2), 210–222.

Fairlie, W. D., Tran, S., & Lee, E. F. (2020). Crosstalk between apoptosis and autophagy signaling pathways. *International Review of Cell and Molecular Biology, 352*, 115–158.

Ferreira, S. S., Passos, C. P., Madureira, P., Vilanova, M., & Coimbra, M. A. (2015). Structure-function relationships of immunostimulatory polysaccharides: A review. *Carbohydrate Polymers, 132*, 378–396.

Frangogiannis, N. (2020). Transforming growth factor-β in tissue fibrosis. *The Journal of Experimental Medicine, 217*(3), Article e20190103.

He, X., Xue, M., Jiang, S., Li, W., Yu, J., & Xiang, S. (2019). Fucoidan promotes apoptosis and inhibits EMT of breast cancer cells. *Biological & Pharmaceutical Bulletin, 42*(3), 442–447.

Henderson, N. C., Rieder, F., & Wynn, T. A. (2020). Fibrosis: From mechanisms to medicines. *Nature, 587*(7835), 555–566.

Hill, C. L., Hunter, D. J., Niu, J., Clancy, M., Guermazi, A., Genant, H., … Felson, D. T. (2007). Synovitis detected on magnetic resonance imaging and its relation to pain and cartilage loss in knee osteoarthritis. *Annals of the Rheumatic Diseases, 66*(12), 1599–1603.

Hinz, B., & Lagares, D. (2020). Evasion of apoptosis by myofibroblasts: A hallmark of fibrotic diseases. *Nature Reviews Rheumatology, 16*(1), 11–31.

Hu, H. H., Chen, D. Q., Wang, Y. N., Feng, Y. L., Cao, G., Vaziri, N. D., & Zhao, Y. Y. (2018). New insights into TGF-β/Smad signaling in tissue fibrosis. *Chemico-Biological Interactions, 292*, 76–83.

Jin, J. O., Song, M. G., Kim, Y. N., Park, J. I., & Kwak, J. Y. (2010). The mechanism of fucoidan-induced apoptosis in leukemic cells: Involvement of ERK1/2, JNK, glutathione, and nitric oxide. *Molecular Carcinogenesis, 49*(8), 771–782.

Junquiera, L. C., Junqueira, L. C., & Brentani, R. R. (1979). A simple and sensitive method for the quantitative estimation of collagen. *Analytical Biochemistry, 94*(1), 96–99.

Kasperkovitz, P. V., Timmer, T. C., Smeets, T. J., Verbeet, N. L., Tak, P. P., van Baarsen, L. G., … Verweij, C. L. (2005). Fibroblast-like synoviocytes derived from patients with rheumatoid arthritis show the imprint of synovial tissue heterogeneity: Evidence of a link between an increased myofibroblast-like phenotype and high-inflammation synovitis. *Arthritis and Rheumatism, 52*(2), 430–441.

Kim, B. S., Kang, H. J., Park, J. Y., & Lee, J. (2015). Fucoidan promotes osteoblast differentiation via JNK- and ERK-dependent BMP2-Smad 1/5/8 signaling in human mesenchymal stem cells. *Experimental & Molecular Medicine, 47*, Article e128.

Lee, H., Kim, J. S., & Kim, E. (2012). Fucoidan from seaweed Fucus vesiculosus inhibits migration and invasion of human lung cancer cell via PI3K-akt-mTOR pathways. *PLoS One, 7*(11), Article e50624.

Li, J., Chen, K., Li, S., Feng, J., Liu, T., Wang, F., … Guo, C. (2016). Protective effect of fucoidan from Fucus vesiculosus on liver fibrosis via the TGF-β1/Smad pathway-mediated inhibition of extracellular matrix and autophagy. *Drug Design, Development and Therapy, 10*, 619–630.

Lin, Y., Qi, X., Liu, H., Xue, K., Xu, S., & Tian, Z. (2020). The anti-cancer effects of fucoidan: A review of both in vivo and in vitro investigations. *Cancer Cell International, 20*, 154.

Luangmonkong, T., Suriguga, S., Mutsaers, H. A. M., Groothuis, G. M. M., Olinga, P., & Boersema, M. (2018). Targeting oxidative stress for the treatment of liver fibrosis. *Reviews of Physiology, Biochemistry and Pharmacology, 175*, 71–102.

Maglaviceanu, A., Wu, B., & Kapoor, M. (2021). Fibroblast-like synoviocytes: Role in synovial fibrosis associated with osteoarthritis. *Wound Repair and Regeneration, 29*(4), 642–649.

Meng, X. M., Nikolic-Paterson, D. J., & Lan, H. Y. (2016). TGF-β: The master regulator of fibrosis. *Nature Reviews. Nephrology, 12*(6), 325–338.

Monsur, H. A., Jaswir, I., Simsek, S., Amid, A., & Alam, Z. (2017). Chemical structure of sulfated polysaccharides from brown seaweed (Turbinaria turbinata). *International Journal of Food Properties, 20*, 1457–1469.

Muñoz-Félix, J. M., González-Núñez, M., & López-Novoa, J. M. (2013). ALK1-Smad1/5 signaling pathway in fibrosis development: Friend or foe? *Cytokine & Growth Factor Reviews, 24*(6), 523–537.

Pradhan, B., Patra, S., Nayak, R., Behera, C., Dash, S. R., Nayak, S., … Jena, M. (2020). Multifunctional role of fucoidan, sulfated polysaccharides in human health and disease: A journey under the sea in pursuit of potent therapeutic agents. *International Journal of Biological Macromolecules, 164*, 4263–4278.

Rasin, A. B., Shevchenko, N. M., Silchenko, A. S., Kusaykin, M. I., Likhatskaya, G. N., Zvyagintseva, T. N., & Ermakova, S. P. (2021). Relationship between the structure of a highly regular fucoidan from Fucus evanescens and its ability to form nanoparticles. *International Journal of Biological Macromolecules, 185*, 679–687.

Remst, D. F., Blaney Davidson, E. N., & van der Kraan, P. M. (2015). Unravelling osteoarthritis-related synovial fibrosis: A step closer to solving joint stiffness. *Rheumatology (Oxford), 54*(11), 1954–1963.

Remst, D. F., Blaney Davidson, E. N., Vitters, E. L., Blom, A. B., Stoop, R., Snabel, J. M., … van der Kraan, P. M. (2013). Osteoarthritis-related fibrosis is associated with both elevated pyridinoline cross-link formation and lysyl hydroxylase 2b expression. *Osteoarthritis and Cartilage, 21*(1), 157–164.

Ryu, M. J., & Chung, H. S. (2016). Fucoidan reduces oxidative stress by regulating the gene expression of HO-1 and SOD-1 through the Nrf2/ERK signaling pathway in HaCaT cells. *Molecular Medicine Reports, 14*(4), 3255–3260.

Sagel, S. D., Khan, U., Jain, R., Graff, G., Daines, C. L., Dunitz, J. M., … Shaffer, M. L. (2018). Effects of an antioxidant-enriched multivitamin in cystic fibrosis. A randomized, controlled, multicenter clinical trial. *American Journal of Respiratory and Critical Care Medicine, 198*(5), 639–647.

Schuster, R., Rockel, J. S., Kapoor, M., & Hinz, B. (2021). The inflammatory speech of fibroblasts. *Immunological Reviews, 302*(1), 126–146.

Shu, Z., Shi, X., Nie, D., & Guan, B. (2015). Low-molecular-weight fucoidan inhibits the viability and invasiveness and triggers apoptosis in IL-1β-treated human rheumatoid arthritis fibroblast synoviocytes. *Inflammation, 38*(5), 1777–1786.

Steenvoorden, M. M., Tolboom, T. C., van der Pluijm, G., Löwik, C., Visser, C. P., DeGroot, J., … Toes, R. E. (2006). Transition of healthy to diseased synovial tissue in rheumatoid arthritis is associated with gain of mesenchymal/fibrotic characteristics. *Arthritis Research & Therapy, 8*(6), R165.

Takeda, K., Tomimori, K., Kimura, R., Ishikawa, C., Nowling, T. K., & Mori, N. (2012). Anti-tumor activity of fucoidan is mediated by nitric oxide released from macrophages. *International Journal of Oncology, 40*(1), 251–260.

Vaamonde-García, C., Flórez-Fernández, N., Torres, M. D., Lamas-Vázquez, M. J., Blanco, F. J., Domínguez, H., & Meijide-Faílde, R. (2021). Study of fucoidans as natural biomolecules for therapeutical applications in osteoarthritis. *Carbohydrate Polymers, 258*, Article 117692.

Vaamonde-García, C., & López-Armada, M. J. (2019). Role of mitochondrial dysfunction on rheumatic diseases. *Biochemical Pharmacology, Jul 165*, 181–195. https://doi.org/10.1016/j.bcp.2019.03.008

Vaamonde-Garcia, C., Malaise, O., Charlier, E., Deroyer, C., Neuville, S., Gillet, P., … de Seny, D. (2019). 15-deoxy-Δ-12, 14-prostaglandin J2 acts cooperatively with prednisolone to reduce TGF-β-induced pro-fibrotic pathways in human osteoarthritis fibroblasts. *Biochemical Pharmacology, 165*, 66–78.

van der Slot, A. J., Zuurmond, A. M., Bardoel, A. F., Wijmenga, C., Pruijs, H. E., Sillence, D. O., … Bank, R. A. (2003). Identification of PLOD2 as telopeptide lysyl hydroxylase, an important enzyme in fibrosis. *The Journal of Biological Chemistry, 278*(42), 40967–40972.

Varone, F., Gibiino, G., Gasbarrini, A., & Richeldi, L. (2019). Evaluation of the lung microbiome as a therapeutic target in the management of idiopathic pulmonary fibrosis: Role of antioxidant/antibiotic combination therapy. *European Review for Medical and Pharmacological Sciences, 23*(14), 6379–6386.

Walton, K. L., Johnson, K. E., & Harrison, C. A. (2017). Targeting TGF-β mediated SMAD signaling for the prevention of fibrosis. *Frontiers in Pharmacology, 8*, 461.

Wang, L., Zhang, P., Li, X., Zhang, Y., Zhan, Q., & Wang, C. (2019). Low-molecular-weight fucoidan attenuates bleomycin-induced pulmonary fibrosis: Possible role in inhibiting TGF-β1-induced epithelial-mesenchymal transition through ERK pathway. *American Journal of Translational Research, 11*(4), 2590–2602.

Wang, W., Chen, H., Zhang, L., Qin, Y., Cong, Q., Wang, P., & Ding, K. (2016). A fucoidan from Nemacystus decipiens disrupts angiogenesis through targeting bone morphogenetic protein 4. *Carbohydrate Polymers, 144*, 305–314.

Watt, F. E., Hamid, B., Garriga, C., Judge, A., Hrusecka, R., Custers, R. J. H., … Vincent, T. L. (2020). The molecular profile of synovial fluid changes upon joint distraction and is associated with clinical response in knee osteoarthritis. *Osteoarthritis and Cartilage, 28*(3), 324–333.

Wu, S. Y., Chen, Y. T., Tsai, G. Y., Hsu, F. Y., & Hwang, P. A. (2020). Protective effect of low-molecular-weight fucoidan on radiation-induced fibrosis through TGF-β1/Smad pathway-mediated inhibition of collagen I accumulation. *Marine Drugs, 18*(3).

Wu, S. Y., Yang, W. Y., Cheng, C. C., Hsiao, M. C., Tsai, S. L., Lin, H. K., … Yuh, C. H. (2020). Low molecular weight fucoidan prevents radiation-induced fibrosis and secondary tumors in a zebrafish model. *Cancers (Basel), 12*(6).

Yamauchi, M., & Sricholpech, M. (2012). Lysine post-translational modifications of collagen. *Essays in Biochemistry, 52*, 113–133.

Yan, S., Yang, B., Shang, C., Ma, Z., Tang, Z., Liu, G., … Zhang, Y. (2016). Platelet-rich plasma promotes the migration and invasion of synovial fibroblasts in patients with rheumatoid arthritis. *Molecular Medicine Reports, 14*(3), 2269–2275.

Yu, X., Zhang, Q., Cui, W., Zeng, Z., Yang, W., Zhang, C., … Luo, D. (2014). Low molecular weight fucoidan alleviates cardiac dysfunction in diabetic goto-kakizaki rats by reducing oxidative stress and cardiomyocyte apoptosis. *Journal Diabetes Research, 2014*, Article 420929.

Zayed, A., El-Aasr, M., Ibrahim, A. S., & Ulber, R. (2020). Fucoidan characterization: Determination of purity and physicochemical and chemical properties. *Marine Drugs, 18*(11).

Zayed, A., & Ulber, R. (2019). Fucoidan production: Approval key challenges and opportunities. *Carbohydrate Polymers, 211*, 289–297.

Zhang, L., Xing, R., Huang, Z., Ding, L., Li, M., Li, X., … Mao, J. (2021). Synovial fibrosis involvement in osteoarthritis. *Frontiers in Medicine (Lausanne), 8*, Article 684389.

Zhang, Y., Du, H., Yu, X., & Zhu, J. (2020). Fucoidan attenuates hyperoxia-induced lung injury in newborn rats by mediating lung fibroblasts differentiate into myofibroblasts. *Annals of Translational Medicine, 8*(22), 1501.

Zhang, Y., Zhao, D., Yang, S., Yao, H., Li, M., Zhao, C., … Wang, F. (2018). Protective effects of fucoidan on epithelial-mesenchymal transition of retinal pigment epithelial cells and progression of proliferative vitreoretinopathy. *Cellular Physiology and Biochemistry, 46*(4), 1704–1715.